CODEN IEJMAT *Internet Electronic Journal of Molecular Design* **2005**, *4*, 647–658 ISSN 1538–6414
BioChem Press http://www.biochempress.com

Inter*net* Electronic Journal of Molecular Design

September 2005, Volume 4, Number 9, Pages 647–658

Editor: Ovidiu Ivanciuc

Proceedings of the Internet Electronic Conference of Molecular Design 2004
IECMD 2004, November 29 – December 12, 2004

syn–2,7–disilatetracyclo[6.2.1.1^{3,6}0^{2,7}]dodec–2(7)–ene: Structural Influence of Incorporation of Disilene into Sesquinorbornene Framework: A DFT Study

Davor Margetić, Mario Vazdar, and Mirjana Eckert–Maksić

Laboratory for Physical Organic Chemistry, Division of Organic Chemistry and Biochemistry, Ruđer Bošković Institute, Bijenička c. 54, 10000 Zagreb, POB 180, Croatia

Received: November 15, 2004; Revised: March 22, 2005; Accepted: May 8, 2005; Published: September 30, 2005

Citation of the article:
D. Margetić, M. Vazdar, and M. Eckert–Maksić, *syn*–2,7–disilatetracyclo[6.2.1.1^{3,6}0^{2,7}]dodec–2(7)–ene: Structural Influence of Incorporation of Disilene into Sesquinorbornene Framework: A DFT Study, *Internet Electron. J. Mol. Des.* **2005**, *4*, 647–658, http://www.biochempress.com.

Inter*net* Electronic Journal of Molecular Design

BioChem Press
http://www.biochempress.com

syn–2,7–disilatetracyclo[6.2.1.1^{3,6}0^{2,7}]dodec–2(7)–ene: Structural Influence of Incorporation of Disilene into Sesquinorbornene Framework: A DFT Study

Davor Margetić,* Mario Vazdar, and Mirjana Eckert–Maksić

Laboratory for Physical Organic Chemistry, Division of Organic Chemistry and Biochemistry, Ruđer Bošković Institute, Bijenička c. 54, 10000 Zagreb, POB 180, Croatia

Received: November 15, 2004; Revised: March 22, 2005; Accepted: May 8, 2005; Published: September 30, 2005

Internet Electron. J. Mol. Des. **2005**, *4* (9), 647–658

Abstract

Motivation. The aim of this computational study was to investigate molecular and electronic structure of disilene embedded in sesquinorbornene skeleton of *syn*–2,7–disilatetracyclo[6.2.1.1^{3,6}0^{2,7}]dodec–2(7)–ene and *anti*–2,7–disilatetracyclo[6.2.1.1^{3,6}0^{2,7}]dodec–2(7)–ene. These novel policyclic systems have not been investigated so far, either experimentally or computationally.

Method. Density functional theory at the B3LYP/6–31G* level was employed.

Results. Quantum chemical calculations of silene and disilene bonds incorporated in sesquinorbornene skeleton using density functional theory at the B3LYP/6–31G* level are reported. Calculated structures of *syn* and *anti* derivatives of disilasesquinorbornenes showed significant non–planarity and asymmetrical deformation of the central Si=Si double bond. The effect of the replacement of the carbon atoms by silicon on molecular and electronic structure of these molecules is discussed.

Conclusions. It was found that replacement of carbon atoms of the central C=C bond by silicon in *syn*– and *anti*–sesquinorbonenes causes significant effects on molecular structure.

Keywords. Pyramidalized alkenes; DFT calculations; sesquinorbornenes; disilenes, silenes.

Abbreviations and notations

DFT, density functional theory	UV, ultraviolet
TMS, tetratmethylsilane	NBO, natural bond orders
FMO, frontier molecular orbital	B3LYP, Becke3 method with Lee, Young and Parr functionals
RHF, restricted Hartree–Fock method	

1 INTRODUCTION

Extensive literature evidence shows that norbornenes (bicyclo[2.2.1]hept–2–enes) have pyramidalized double bond with hydrogen atoms bent in the *endo* direction [1–3]. The *syn*–sesquinorbornenes exhibit almost twice as much bending of the central π bond [4]. There are

Presented in part at the Internet Electronic Conference of Molecular Design 2004, IECMD 2004.

* Correspondence author; phone: 385–1–4561–008; fax: 385–1–4680–195; E–mail: margetid@emma.irb.hr.

several theoretical papers dealing with pyramidalization in sesquinorbornenes and related policyclic systems [5]. While all–carbon sesquinorbornenes are studied in detail, both experimentally and theoretically, hetero–sesquinorbornenes have not attracted much attention [6–9]. All studies published so far are dealing with replacement of carbon bridge (C_{11} and C_{12}) with heteroatoms, while molecular and electronic structures of sesquinorbornenes possessing heteroatoms at the central double bonds have not been investigated so far.

Molecular structure of disilenes exhibits some interesting features. It is known experimentally that double bonds in disilenes and digermenes ($R_2M=MR_2$, M=Si, Ge) [10–13] are non–planar ($\Psi > 0^o$) and that there is a twist (τ) around the double bond, in which two organometallic atoms are pyramidalized in *anti* fashion (Chart 1)[14,15]. It was also shown, both experimentally [16–18] and theoretically [19–23] that the degree of disilene bond bending strongly depends on the nature of substituents. In this regard, it should be noted that carbon (tetraalkyl) substituted disilenes generally adopt *trans*– bent structures with C_{2h} symmetry (planar structure of disilene possess D_{2h} symmetry) [20]. Furthermore, a slight twisting around the double bond by the angle τ may also occur in order to reduce steric overcrowding. The observed disilene bond deviations from planarity were attributed to hyperconjugative interactions between the Si=Si π bond and σ orbitals of the appropriate symmetry on the substituents. Kira and co–workers assumed that the same electronic effects play an important role in defining geometries of digermene structures [24].

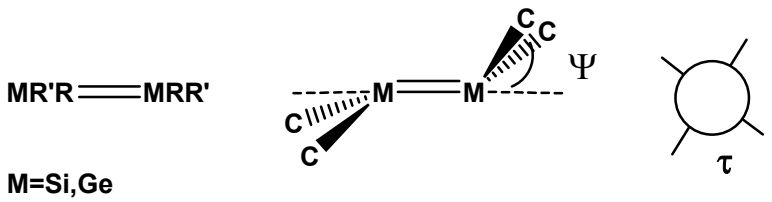

Chart 1.

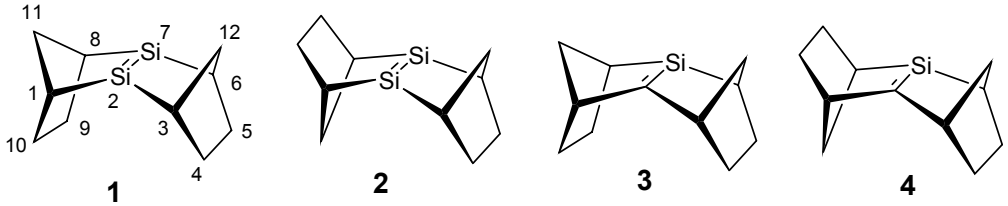

Chart 2.

To the best of our knowledge, the influence of replacement of the olefinic carbon atoms in sesquinorbornene with the IVA group elements on the extent of double bond bending, has not been yet studied computationally. The aim of this computational study is to explore molecular and

electronic structure of disilene embedded in the sesquinorbornene skeleton (Chart 2). Both *syn*–2,7–disilatetracyclo[6.2.1.1^{3,6}0^{2,7}]dodec–2(7)–ene (**1**) and *anti*–2,7–disilatetracyclo[6.2.1.1^{3,6}0^{2,7}] dodec–2(7)–ene (**2**) systems were calculated. It was anticipated that rigid and strained norbornene skeleton influences the flexibility of disilene bending, favoring *syn* fashion. In addition, calculations for related silenes, *syn*–2–silatetracyclo[6.2.1.1^{3,6}0^{2,7}]dodec–2(7)–ene (**3**) and *anti*–2–silatetracyclo[6.2.1.1^{3,6}0^{2,7}]dodec–2(7)–ene (**4**) were carried out for the sake of completeness.

2 MATERIALS AND METHODS

All geometry optimizations were carried out with the *Gaussian 98* suite of programs [25] employing the density functional theory (DFT) hybrid B3LYP method using 6–31G* basis set [26,27]. This method has been demonstrated to describe correctly the structures of a variety of silanes and disilanes in literature [28]. The natures of the stationary points were characterized by the vibrational frequency calculations. Hyperconjugative interactions were quantified using the NBO methodology of Weinhold and coworkers [29]. All calculations were conducted on the dual Athlon MP and Pentium III personal computers under the Linux Redhat 8.0 operating system.

3 RESULTS AND DISCUSSION

The B3LYP/6–31G* optimized geometries of molecules **1**–**4** are shown in Figures 1–4. Their total energies and selected geometrical parameters are collected in Table 1, while Table 2 lists orbital interaction parameters.

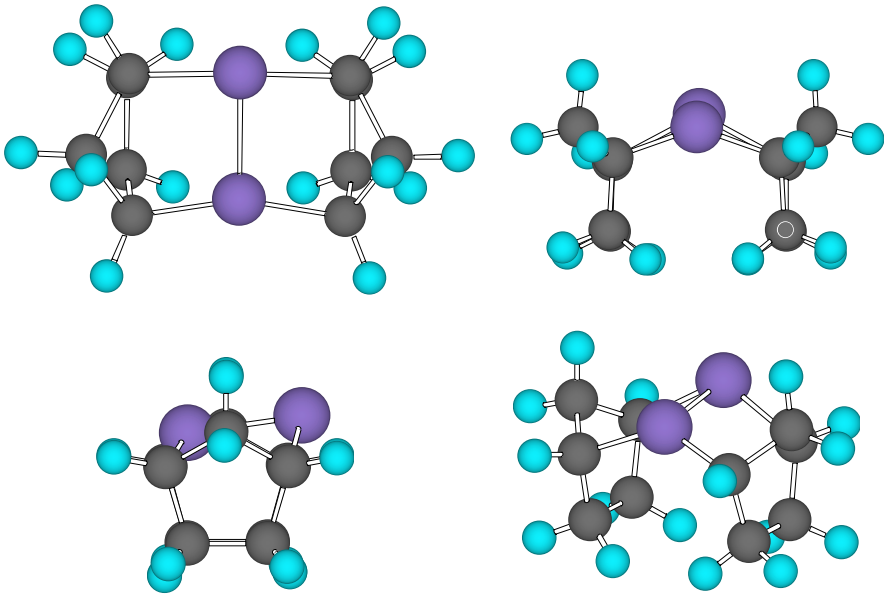

Figure 1. B3LYP optimized structure of **1**.

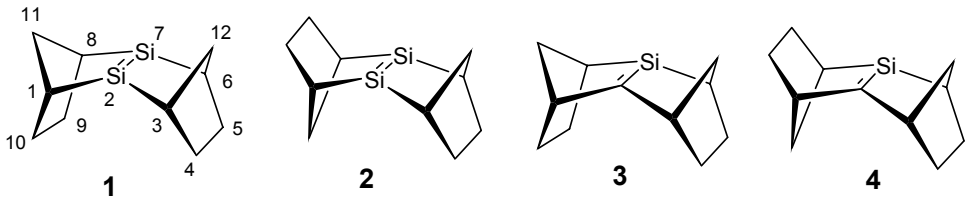

Table 1. Selected B3LYP/6–31G* geometrical parameters and total energies of molecules **1**–**4**

Distance /Å	**1**	**2**	**3**	**4**
M_2M_7	2.244	2.280	1.778	1.789
C_1M_2/C_3M_2	1.909	1.905/1.907	1.500	1.511/1.492
C_8M_7/C_6M_7	2.075	2.103/2.068	1.969	1.970/1.981
C_1C_{10}/C_3C_4	1.561	1.560/1.553	1.576	1.558/1.579
C_8C_9/C_5C_6	1.552	1.549/1.558	1.559	1.561/1.556
C_1C_{11}/C_3C_{12}	1.546	1.550/1.558	1.555	1.568/1.549
C_8C_{11}/C_6C_{12}	1.555	1.543/1.554	1.553	1.556/1.549
C_9C_{10}/C_4C_5	1.558	1.560/1.566	1.556	1.555/1.565
Angle / ^{o}				
$C_1M_2C_3$	131.8	123.2	133.9	129.5
$C_6M_7C_8$	121.5	112.5	138.9	132.6
$C_1M_2M_7$ /$C_3M_2M_7$	105.9	107.8/108.3	111.6	112.4/112.5
$C_8M_7M_2/C_6M_7M_2$	78.7	75.3/73.6	88.1	87.1/86.6
$C_1C_{11}C_8/C_3C_6C_{12}$	100.5	99.5/100.0	98.9	97.9/98.7
Dihedral angle / ^{o}				
$C_1M_2M_7C_3$	143.2	135.3	163.5	156.2
$C_6M_7M_2C_8$	125.7	126.0	138.9	133.0
Butterfly bending / ^{o}				
Ψ_2	36.8	44.7	16.5	23.8
Ψ_7	54.3	54.0	41.1	47.0
E_{tot}/a.u.	–969.581825	–969.580735	–718.205661	–718.196085

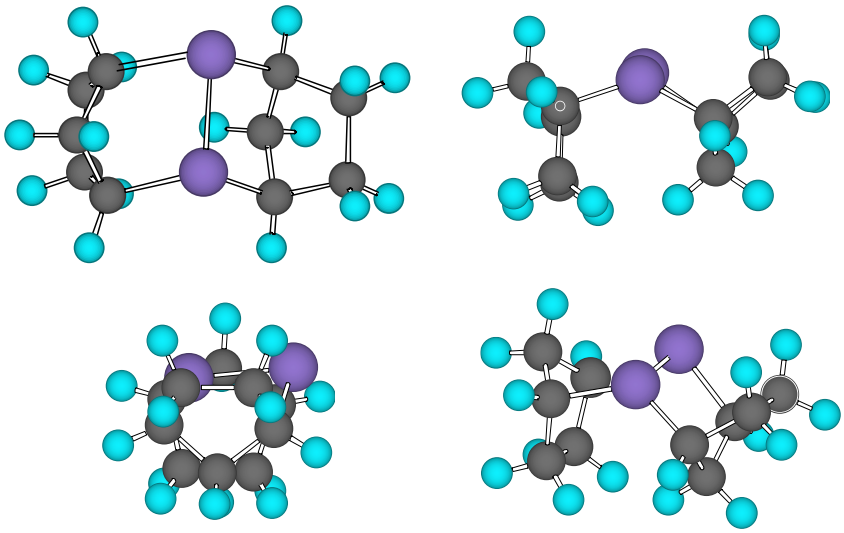

Figure 2. B3LYP optimized structure of **2**.

Table 2. RHF/6–31G*//B3LYP/6–31G* NBO orbital interaction parameters for molecules **1** and **2**

1	**2**
$\pi(Si_2Si_7)\rightarrow\sigma^*(C_6H_6)$ (2.61)	$\pi(Si_2Si_7)\rightarrow\sigma^*(C_6H_6)$ (4.48)
$\pi(Si_2Si_7)\rightarrow\sigma^*(C_3H_3)$ (1.12)	$\pi(Si_2Si_7)\rightarrow\sigma^*(C_3H_3)$ (0.65)
	$\sigma(C_9H_{10})\rightarrow\pi^*(Si_2Si_7)$ (0.61)
	$\sigma(C_3C_4)\rightarrow\pi^*(Si_2Si_7)$ (0.61)
	$\pi(Si_2Si_7)\rightarrow\sigma^*(C_8H_8)$ (2.34)
	$\pi(Si_2Si_7)\rightarrow\sigma^*(C_3H_3)$ (2.09)
	$\pi(Si_2Si_7)\rightarrow\sigma^*(C_9H_9)$ (0.69)
	$\pi(Si_2Si_7)\rightarrow\sigma^*(C_{10}H_{10})$ (0.65)
	$LP(Si_7)\rightarrow\sigma^*(C_8C_9)$ (2.82)
	$LP(Si_2)\rightarrow\sigma^*(C_1C_{10})$ (0.63)
	$LP(Si_7)\rightarrow\sigma^*(C_6C_{12})$ (4.33)
	$LP(Si_2)\rightarrow\sigma^*(C_3C_{12})$ (0.63)
$\pi(Si_2Si_7)\rightarrow\sigma^*(C_1Si_2)$ (9.57)	$\sigma(C_3C_{12})\rightarrow LP^*(Si_2)$ (6.41)
$\pi(Si_2Si_7)\rightarrow\sigma^*(C_6Si_7)$ (5.12)	$LP(Si_2)\rightarrow\pi^*(Si_2Si_7)$ (4.70)
$LP^*(Si_2)\rightarrow\pi^*(Si_2Si_3)$ (4.54)	$\sigma(Si_7C_8)\rightarrow LP^*(Si_2)$ (36.88)
$\sigma(C_6Si_7)\rightarrow LP^*(Si_2)$ (27.81)	$\sigma(C_6Si_7)\rightarrow LP^*(Si_2)$ (29.33)
$\sigma(C_1Si_2)\rightarrow\sigma^*(Si_2C_3)$ (10.75)	$\pi(Si_2Si_7)\rightarrow\sigma^*(Si_2C_3)$ (12.70)
$\sigma(Si_2C_3)\rightarrow\sigma^*(C_1Si_2)$ (10.75)	$\pi(Si_2Si_7)\rightarrow\sigma^*(Si_2C_1)$ (13.81)
	$\sigma(Si_2C_3)\rightarrow\sigma^*(Si_2C_1)$ (10.59)
	$\sigma(Si_2C_{10})\rightarrow\sigma^*(Si_2C_3)$ (10.18)
	$\pi(Si_2Si_7)\rightarrow\sigma^*(Si_7C_8)$ (5.86)
	$\pi(Si_2Si_7)\rightarrow\sigma^*(Si_7C_6)$ (3.88)
$\pi(Si_2Si_7)\rightarrow\sigma^*(C_{11}H_{11out})$ (2.48)	$\pi(Si_2Si_7)\rightarrow\sigma^*(C_{11}H_{11out})$ (2.12)
	$\sigma(Si_2C_3)\rightarrow\sigma^*(C_{12}H_{12out})$ (5.61)
	$\sigma(Si_2C_{10})\rightarrow\sigma^*(C_{11}H_{11out})$ (6.21)

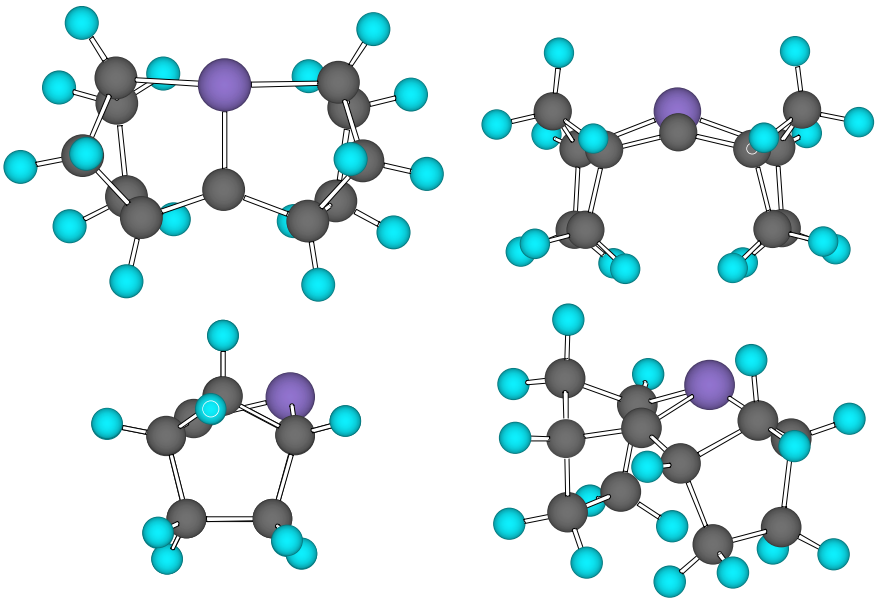

Figure 3. B3LYP optimized structure of **3**.

Molecular structure. As depicted in Figures 1 and 2, structures of molecules **1** and **2** have C_1 symmetry, while *syn*– and *anti*–sesquinorbornenes have higher, C_{2v} and C_{2h} symmetry, respectively. Remarkable large butterfly bending values were found in both structures **1** and **2**: 36.1° and 54.3° at

the Si_2 and Si_7 atoms in molecule **1**, while for molecule **2** corresponding values are 44.7° and 54.0° (Table 1) [30]. There are only a few examples of comparably large pyramidalized sesquinorbornenes reported in literature [31]. However, the computed extent of butterfly bending in molecules **1** and **2** is much larger than the most pyramidalized disilenes reported so far (tetramesityl disilene Ψ = 33.8°) [32] Similar large extent of butterfly bending was found for related molecules **3** and **4** (Figures 3 and 4), where silene is incorporated in sesquinorbornene moiety. In *syn*– molecule **3**, butterfly bending at the silicon atom is (Ψ_{Si2} = 41.1°, while pyramidalization at the carbon atom is of similar magnitude to that previously reported for *syn*–sesquinorbornenes (Ψ_{C7} = 16.5°). Somewhat surprisingly, larger pyramidalizations are found in *anti*– isomer **4** (Ψ_{Si2} = 47.0° and Ψ_{C7} = 25.1°). We assume that the observed deformation of the double bond in the considered disilenes reflects tendency of the occupied *p*–orbitals of the silene fragments to minimize repulsive interactions.

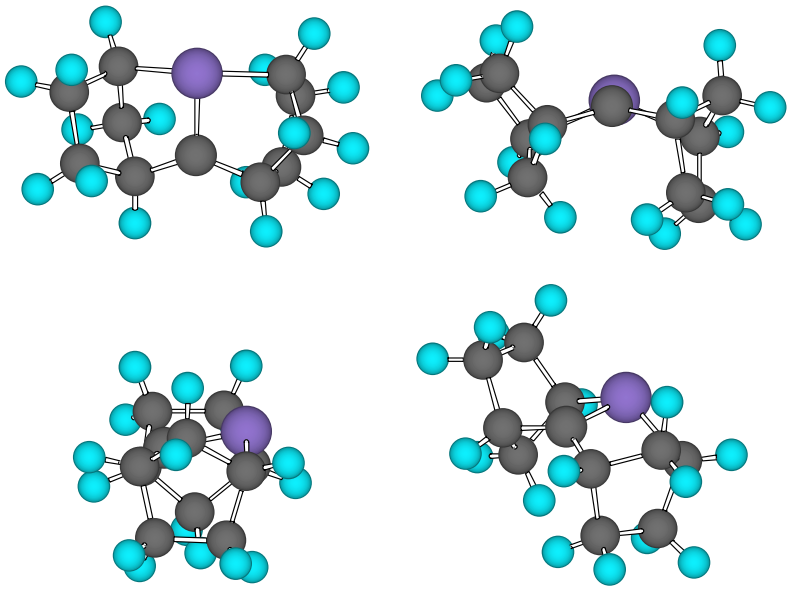

Figure 4. B3LYP optimized structure of **4**.

Other important structural features include twisting angle, C–Si–C angles and the length of the central double bond. Both structures show minimal twisting angle (τ) between two silicon atoms, due to geometrical constraints imposed by sesquinorbornene skeleton. Furthermore, calculated C–Si–C angles for molecules **1**–**4** are significantly larger than experimental ones (the range is 112.5–116.8°). The B3LYP calculated lengths of the Si_2=Si_7 central double bond in **1** and **2** are 2.244 and 2.280 Å, respectively. These lengths are within the range of experimentally measured values for various disilenes (2.143–2.260 Å) [16–18]. Comparison of these structures with calculated structure of corresponding disilanorbornene, *i.e.* 2,3–disilatricyclo[2.2.1]hept–2–ene, revealed similar

geometrical features around the Si=Si bond and double bond hydrogen *trans*– twisting.

Energetics. Calculations revealed that *syn* **1** is by 4.86 kJ mol^{-1} energetically more stable than *anti* **2**. This is significantly smaller than previously calculated for *syn/anti*–dioxa and *syn/anti*–sesquinorbornene pairs at the same level of theory, (6.1 and 10.7 kJ mol^{-1}, respectively) [8]. Calculated difference may be associated with the fact that *anti*–sesquinorbornene and *anti*–dioxasesquinorbornene have planar structures, while their *syn* counterparts are pyramidalized. In contrast, energy difference between **3** and **4** is calculated to be much larger, *i.e.*, 25.1 kJ mol^{-1}.

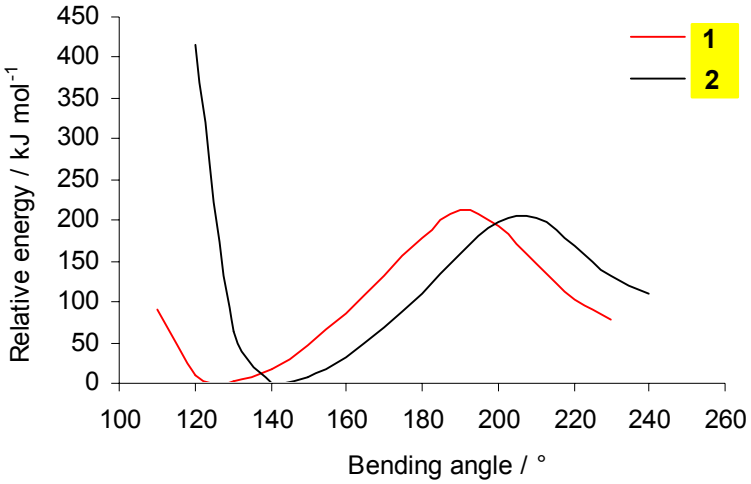

Figure 5. Torsional energy surfaces for compounds **1** and **2**.

Torsional energy surfaces for compounds **1** and **2** (Figure 5) were obtained by single– point energy calculation at each point of the scan (with 10° increment, going from the *endo* to the *exo* bending). Both species have energy minima with the π–bond butterfly bending towards *endo* face of the norbornene skeleton, in addition to the energy maximum structure at Ψ = 190° and 200°, respectively [33].

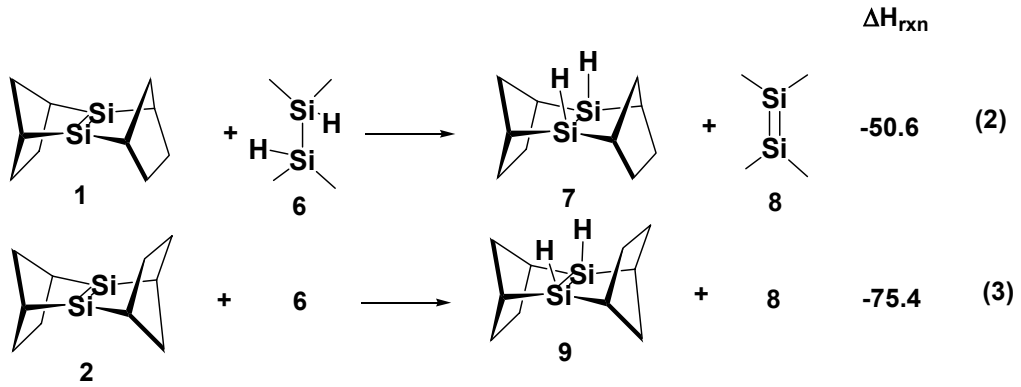

Scheme 1.

Furthermore, olefin strain energies (OSE) for molecules **1** and **2** were calculated as a difference between the energy of hydrogenation of the alkene and the heat of hydrogenation of the

corresponding unstrained alkene (Eq. 1) [34,35].

$$OSE=\Delta H_{hydrog}(\text{strained alkene}) - \Delta H_{hydrog}(\text{unstrained alkene}) \quad (1)$$

Relative OSE of molecules **1** and **2** were obtained according to Eq. (2) and (3), where tetramethyldisilene was used as reference (Scheme 1). Calculations at B3LYP/6–31G* level indicate that *anti*– isomer **2** has larger OSE than **1** by 24.8 kJ mol^{-1}, indicating that **2** is much more strained.

Electronic structure. The energy levels of the σ–bonds of disilenes are raised by the ring strain. Accordingly, the stereo–electronic interactions between the strained CC σ bonds and the SiSi π bond become effective. The UV/VIS absorption maximum of the π–π* transition in strained disilenes is 493 nm [36]. This indicates that the transition is red–shifted relative to the typical values for tetraalkyl disilenes (400–470 nm) [37]. This remarkable shift is mainly due to the lengthening and twisting of the central double bond. Calculations of the orbital energies at the RHF/6–31G*//B3LYP/6–31G* level have shown that HOMO and LUMO energies for **1** are –6.82 and 0.84 eV, whereas for *anti*– isomer **2** the corresponding frontier molecular orbital energy values are –7.24 and 0.89 eV, respectively [38]. HOMO of *syn*–disilasesquinorbornene **1** has electron density mainly located on silicon atom Si_7, with considerable contribution of σ character associated with the C_5C_6 and C_8C_9 bonds (Figure 6). On the contrary, LUMO has electron density mainly located on silicon Si_6, and substantial contributions from the σ hyperconjugative interactions with σ orbitals of the C_3C_4 and C_1C_{10} bonds.

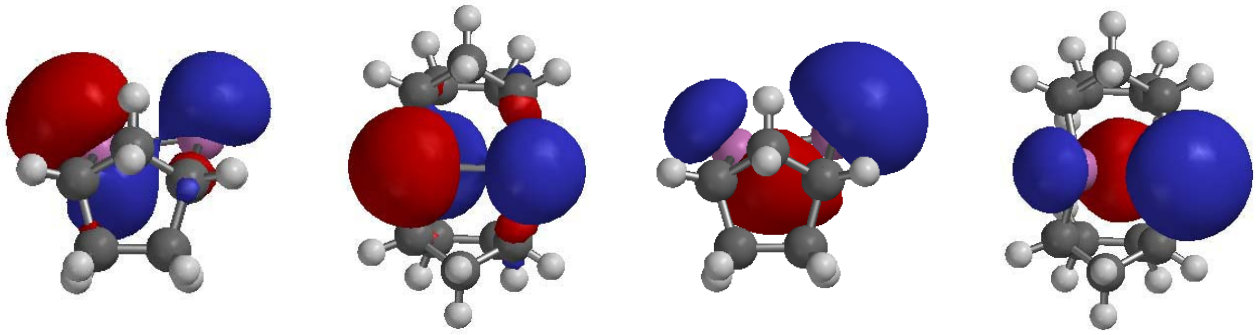

LUMO HOMO

Figure 6. FMOs of molecule **1**.

Figure 7 depicts FMO of *anti* isomer **2**. Here, in both orbitals, the electron density is mainly localized on Si_7. Difference in FMO gap between **1** and **2** is reflected in their calculated π–π* transitions. For molecule **1** π–π* transition wavelength was calculated by using the TDDFT method [39] to be 576.5 nm, while for *anti* isomer **2** somewhat higher value of 587.9 nm was obtained. It is also interesting to note that the calculated HOMO–LUMO gap in **1** and **2** is considerably smaller than in the corresponding hydrocarbons (B3LYP/6–31G* values for **1** and **2** are 2.79 and 2.88 eV, respectively, while *syn*– and *anti*–sesquinorbornene FMO gaps are 6.47 and 6.36 eV). These smaller FMO differences indicate that their kinetic stability is significantly lower [40].

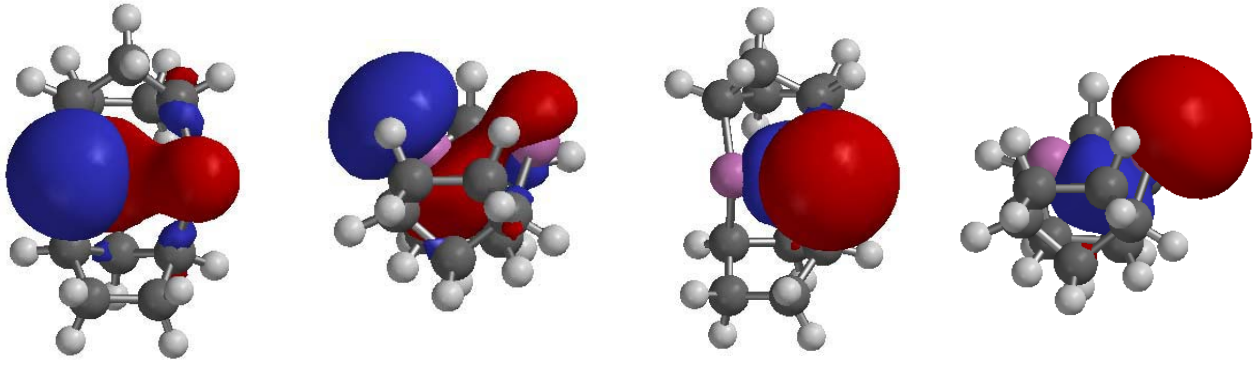

LUMO HOMO

Figure 7. FMOs of molecule **2**.

Table 3. RHF/6–31G*//B3LYP/6–31G* NBO orbital interaction parameters for molecules **1–symm**, **3** and **4**

1–symm [a]	**3**	**4**
$\pi(Si_2Si_7)\rightarrow\sigma^*(C_5C_6)$ (2.04)	$\pi(C_2Si_7)\rightarrow\sigma^*(C_3C_4)$ (3.20)	$\pi(C_2Si_7)\rightarrow\sigma^*(C_8H_8)$ (2.36)
$\pi(Si_2Si_7)\rightarrow\sigma^*(C_6H_6)$ (1.06)	$\pi(C_2Si_7)\rightarrow\sigma^*(C_3H_3)$ (3.55)	$\pi(C_2Si_7)\rightarrow\sigma^*(C_1H_1)$ (6.65)
$\sigma(C_4H_4)\rightarrow\sigma^*(Si_2C_3)$ (4.46)	$\pi(C_2Si_7)\rightarrow\sigma^*(C_8C_9)$ (1.50)	$\pi(C_2Si_7)\rightarrow\sigma^*(C_3C_{12})$ (1.21)
$\sigma(C_1C_{11})\rightarrow\sigma^*(C_8H_8)$ (4.07)	$\pi(C_2Si_7)\rightarrow\sigma^*(C_8H_8)$ (1.83)	$\pi(C_2Si_7)\rightarrow\sigma^*(C_8C_{11})$ (0.84)
	$\sigma(C_1H_1)\rightarrow\pi^*(C_2Si_7)$ (2.00)	$\pi(C_2Si_7)\rightarrow\sigma^*(C_{12}H_{12out})$ (1.62)
$\pi(Si_2Si_7)\rightarrow\sigma^*(C_6C_{12})$ (0.63)	$\sigma(C_3H_3)\rightarrow\sigma^*(C_3C_{12})$ (1.46)	$\sigma(C_7C_8)\rightarrow\sigma^*(C_2C_3)$ (3.57)
	$\sigma(C_2C_3)\rightarrow\sigma^*(C_1C_{11})$ (0.69)	$\sigma(C_8C_9)\rightarrow\pi^*(C_2Si_7)$ (1.50)
	$\sigma(C_3C_{12})\rightarrow\sigma^*(C_1C_2)$ (4.71)	$\sigma(C_1H_1)\rightarrow\pi^*(C_2Si_7)$ (3.05)
	$\sigma(C_3C_{12})\rightarrow\pi^*(C_2Si_7)$ (0.51)	$\sigma(C_3C_{12})\rightarrow\sigma^*(C_1C_2)$ (4.12)
	$\sigma(C_3C_{12})\rightarrow\sigma^*(C_6H_6)$ (2.46)	$\sigma(C_{12}H_{12in})\rightarrow\pi^*(C_2Si_7)$ (1.94)
$\sigma(C_1Si_2)\rightarrow\sigma^*(Si_2C_3)$ (10.39)	$\pi(C_2Si_7)\rightarrow\sigma^*(C_6Si_7)$ (8.94)	$\pi(C_2Si_7)\rightarrow\sigma^*(C_6Si_7)$ (1.31)
$\sigma(C_{11}C_{11out})\rightarrow\sigma^*(C_1Si_2)$ (3.26)	$\sigma(C_2C_3)\rightarrow\sigma^*(C_{12}H_{12out})$ (1.59)	$\sigma(C_6C_7)\rightarrow\sigma^*(C_{12}H_{12out})$ (5.87)
$\sigma(C_1C_{10})\rightarrow\sigma^*(C_{11}H_{11in})$ (3.26)	$\sigma(C_3C_4)\rightarrow\sigma^*(C_{12}H_{12in})$ (2.59)	$\sigma(C_7C_8)\rightarrow\sigma^*(C_{11}H_{11out})$ (3.57)

[a] molecule **1** with forced C_s symmetry, C–Si and Si=Si bonds lengths constrained to 2.060 Å and 2.240 Å, and pyramidalization angle constrained to 15°.

Table 4. RHF/6–31G*//B3LYP/6–31G* NBO orbital interaction parameters for molecules **1a** and **5**

1a [a]	**5**
$\pi(Si_2Si_7)\rightarrow\sigma^*(C_3C_4)$ (1.99)	$\pi(C_2C_7)\rightarrow\sigma^*(C_3C_4)$ (3.38)
$\pi(Si_2Si_7)\rightarrow\sigma^*(C_1H_1)$ (7.21)	$\pi(C_2C_7)\rightarrow\sigma^*(C_1H_1)$ (1.33)
$\sigma(C_1C_{10})\rightarrow\pi^*(Si_2Si_7)$ (1.55)	$\sigma(C_1C_{10})\rightarrow\pi^*(C_2C_7)$ (3.40)
$\sigma(C_1H_1)\rightarrow\pi^*(Si_2Si_7)$ (0.56)	$\sigma(C_2C_3)\rightarrow\sigma^*(C_7C_8)$ (3.45)
$\sigma(C_1C_{11})\rightarrow\sigma^*(Si_2C_3)$ (9.33)	$\sigma(C_1C_{11})\rightarrow\sigma^*(C_2C_3)$ (5.90)
$\sigma(C_1C_{11})\rightarrow\sigma^*(Si_2Si_7)$ (3.22)	$\sigma(C_1C_{11})\rightarrow\sigma^*(C_1H_1)$ (3.27)
$\sigma(C_1Si_2)\rightarrow\sigma^*(Si_7C_6)$ (8.13)	
$\pi(Si_2Si_7)\rightarrow\sigma^*(C_{11}H_{11out})$ (3.84)	$\pi(C_2C_7)\rightarrow\sigma^*(C_{11}H_{11out})$ (0.79)
	$\sigma(C_6C_7)\rightarrow\sigma^*(C_{12}H_{12out})$ (2.02)
	$\sigma(C_8C_9)\rightarrow\sigma^*(C_{11}H_{11in})$ (2.44)

[a] geometry of **5** used, C=C atoms replaced by Si=Si without optimization.

Tables 2–4 list NBO interaction parameters for the studied molecules. An inspection of these results shows that $\pi\rightarrow\sigma^*$ hyperconjugative interactions in the series of molecules studied are almost absent. This result is in contrast with previous calculations showing that $\pi(C_2C_7)\rightarrow\sigma^*(C_5C_6)$ and $\pi(C_2C_7)\rightarrow\sigma^*(C_6C_{12})$ interactions are dominant in *syn*–sesquinorbornene and *syn*–dioxasesquinorbornene [41]. Our calculations indicate that elongation of the Si_2Si_7 and C_1Si_2 bonds

greatly diminishes these interactions in molecules **1** and **2**. Instead, interactions of double bond with bridge hydrogen σ bonds, ($\pi(Si_2Si_7)\rightarrow\sigma^*(C_6H_6)$) are much larger. The strongest interactions are calculated to be these of σ bonds with LP like p–orbital of silicon atom: $\sigma(C_6Si_7)\rightarrow LP^*(Si_2)$ and $\sigma(Si_2C_3)\rightarrow\sigma^*(C_1Si_2)$ interactions. Furthermore, $\pi\rightarrow\sigma^*$ interactions of the central double bond with bridgehead hydrogens have been detected $\pi(Si_2Si_7)\rightarrow\sigma^*(C_{11}H_{11out})$. Interactions of identical nature and of similar extent were found also in a hypothetical molecule **1symm**. In this structure, C_s symmetry was imposed and C–Si and Si=Si bonds lengths constrained to 2.060 Å and 2.240 Å, respectively, while pyramidalization angle was constrained to 15°. This indicates that replacement of the C=C bridge with the Si=Si bond causes significant changes in the nature of the orbital interactions within a molecule. Further insight into electronic structure of disilene **1** was obtained by analysis of disila–*syn*–sesquinorbornene molecule **1a**. In this hypothetical molecule, optimized geometry of **5** was used, and C=C atoms were replaced by Si=Si without geometry optimization, thus forming disilene **1** possessing geometry of **5**. In both molecules (**1** and **1a**), similar orbital interactions of comparable size were found. This result indicates that difference in orbital interactions between **1** and **5** are caused mainly by different geometries and double bond elongation, rather than by replacement of carbon by silicon atom. Finally, for molecules **3** and **5** similar hyperconjugative interactions were found, as would be expected, due to a greater similarity of these two structures.

Chemical shifts. Due to asymmetry of the considered molecules, two silicon atoms possess different ^{29}Si NMR chemical shifts. The GIAO/B3LYP/6–31G*//B3LYP/6–31G* nuclear magnetic shielding tensors calculated for molecule **1** are estimated to be 188.5 and –124.8 ppm for Si_2 and Si_7, respectively, while in **2** the corresponding values are 260.1 and –171.5 ppm. The δ^{29}Si NMR values are 225.9 and 539.3 ppm for **1**, while 154.4 and 585.9 ppm for **2**, relative to TMS. δ^{29}Si(TMS) is calculated as 414.3 ppm [42]. For a comparison, δ^{29}Si for $Me_2Si{=}SiMe_2$ calculated at the same level of theory amounts 278.9 ppm. These results indicate unusual magnetic environment around disilene bond in **1** and **2** as compared with available experimental data for distorted disilenes [43].

4 CONCLUSIONS

Density functional calculations have been carried out to estimate the effect of replacing central C=C bridge with the silene (C=Si) and disilene (Si=Si) double bond on geometry of sesquinorbornene molecular framework. This results in large distortion of the molecular structure and considerable increase in pyramidalization angles relative to sesquinorbornene, as well as to a large butterfly bending. It is also shown that hyperconjugative interactions between the central double bond and norbornene σ skeleton are greatly diminished.

Acknowledgment

This work was supported by Croatian Ministry of Science, Education and Sport through the Projects Nos. 0098147 and 0098056.

5 REFERENCES

[1] W. T. Borden, Pyramidalized Alkenes, *Chem. Rev.* **1989**, *89*, 1095–1109.
[2] P. A. Carrupt and P. Vogel, Double Bond Pyramidalization in Bicyclic Alkanes. *Ab Initio* MO Calculations on Bicyclo[2.2.1]hept–2–ene, Bicyclo[2.1.1]hex–2–ene and Bicyclo[3.2.1]oct–6–ene Derivatives. *J Mol Struct (THEOCHEM)* **1985**, *124*, 9–23.
[3] W. Luef and R. Keese, Strained Olefins: Structure and Reactivity of Nonplanar Carbon–Carbon Double Bonds, *Topics in Stereochemistry* **1991**, *20*, 231–318.
[4] IUPAC name for sesquinorbornene: tetracyclo[6.2.1.1^{3,6}0^{2,7}]dodec–2(7)–ene, the numbering system used in this paper follows IUPAC rules.
[5] M. C. Holthausen and W. Koch, Double–Bond Geometry in Norbornene, Sesquinorbornenes, and Related Compounds. A High–Level Quantum Chemical Investigation, *J. Phys. Chem.* **1993**, *97*, 10021–10027 and references cited therein.
[6] J. Spanget–Larsen and R. Gleiter, Structure and Reactivity of Norbornene and syn–Sesquinorbornene, *Tetrahedron* **1983**, *39*, 3345–3350.
[7] I. Antol, M. Eckert–Maksić, D. Margetić, Z. B. Maksić, K. Kowski and P. Rademacher, Electronic and Molecular Structural Study of 7,7'–dioxasesquinorbornenes, *Eur. J. Org. Chem.* **1998**, 1403–1408.
[8] D. Margetić, M. Eckert–Maksić, I. Antol, Z. Glasovac and R. N. Warrener, A DFT Study of Pyramidalized Alkenes: 7–Oxasesquinorbornenes and 7,7'–Dioxasesquinorbornenes, *Theor. Chem. Acc.* **2003**, *109*, 182–189.
[9] M. Eckert–Maksić, I. Antol, D. Margetić and Z. Glasovac, *syn*–Sesquinorbornenyl Carbocations and Their Boron Analogues. *Ab Initio* and DFT Study, *J. Chem. Soc. Perkin 2* **2002**, 2057–2063.
[10] J. T. Snow, S. Murakami, S. Masamune and D. J. Williams, Synthesis and Characterization of Tetrakis(2,6–diethylphenyl)digermene, *Tetrahedron Lett.* **1984**, *25*, 4191–4194.
[11] N. Tokitoh, K. Kishikawa, R. Okazaki, T. Sasamori, N. Nakata and N. Takeda, Synthesis and Characterization of an Extremely Hindered Tetraaryl–substituted Digermene and its Unique Properties in the Solid State and in Solution, *Polyhedron* **2002**, *21*, 563–577.
[12] M. Weidenbruch, M. Sturmann, H. Kilian, S. Pohl and W. Saak, A Tetraaryldigermene with a Short Germanium–Germanium Double Bond and a Nearly Planar Environment of Both Germanium Atoms, *Chem. Ber.–Recueil* **1997**, *130*, 735–738.
[13] M. Stender, L. H. Pu and P.P. Power, Stabilized Terphenyl–Substituted Digermene Derivatives of Simple Organic Groups and Their Halide Precursors: Preference for Symmetrically Bonded Structures, *Organometallics* **2001**, 124, 1820–1824.
[14] Y. Apeloig, in *The chemistry of organic silicon compounds*, S. Patai and Z. Rappoport, eds., Wiley, Chichester **1989**, p. 57.
[15] M. Driess and H. Grützmacher, Main Group Element Analogues of Carbenes, Olefines, and Small Rings, *Angew. Chem. Int. Ed. Engl.* **1996**, *35*, 828–856.
[16] S. Matsumoto, S. Tsutsui, E. Kwon and K. Sakamoto, Formation of a Stable, Lattice–Framework Disilene: A Strategy for the Construction of Bulky Substituents, *Angew. Chem. Int. Ed. Engl.* **2004**, *43*, 4610–4612.
[17] M. Kira, T. Maruyama, C. Kabuto, K. Ebata and H. Sakurai, Stable Tetrakis(triarylsilyl)disilenes; Synthesis, X–Ray Structures, and UV/VIS Spectra, *Angew. Chem. Int. Ed. Engl.* **1994**, *33*, 1489–1491.
[18] M. Kira, S. Ohya, T. Iwamoto, M. Ichinohe and C. Kabuto, Facile Rotation around Si=Si Double Bonds in Tetrakis(trialkylsilyl)disilenes, *Organometallics* **2000**, *19*, 1817–1819.
[19] W.–C. Chen, M.–D. Su and S.–Y. Chu, Substituents Effects on Shape Deformation and Energies of the Silicon and Germanuim Double Bond, *Organometallics* **2001**, *20*, 564–567.
[20] L. Sari, M.C. McCarthy, H. F. Schaefer III and P. Thaddeus, Mono– and Dibridged Isomers of Si2H3 and Si2H4: the True Ground State Global Minima. Theory and Experiment in Concert, *J. Am. Chem. Soc.* **2003**, *125*, 11409–11417.
[21] C. Liang and L.C. Allen, Group IV Double Bonds: Shape Deformation and Substituent Effects, *J. Am. Chem. Soc.* **1990**, *112*, 1039–1041.
[22] M. Karni and Y. Apeloig, Substituent Effects on the Geometries and Energies of the Si=Si Double Bond, *J. Am. Chem. Soc.* **1990**, *112*, 8589–8590.
[23] H. Jacobsen and T. Ziegler, Nonclassical Double Bonds in Ethylene Analogues: Influence of Pauli Repulsion on Trans Bending and π–Bond Strength. A Density Functional Study, *J. Am. Chem. Soc.* **1994**, *116*, 3667–3679.

[24] M. Kira, T. Iwamoto, T. Maruyama, C. Kabuto and H. Sakurai, Tetrakis(trialkylsilyl)digermenes. Salient Effects of Trialkylsilyl Substituents on Planarity Around the Ge=Ge Bond and Remarkable Thermochromism, *Organometallics* **1996**, *15*, 3767–3769.
[25] Gaussian 98, Revision A.5, M.J. Frisch, G.W. Trucks, H.B. Schlegel, G.E. Scuseria, M. Robb, J.R. Cheeseman, V.G. Zakrzewski, J.A. Montgomery Jr., R.E. Stratmann, J.C. Burant, S. Dapprich, J.M. Millam, A.D. Daniels, K.N. Kudin, M.C. Strain, O. Farkas, J. Tomasi, V. Barone, M. Cossi, R. Cammi, B. Mennucci, C. Pomelli, C. Adamo, S. Clifford, J. Ochterski, G.A. Petersson, P.Y. Ayala, Q. Cui, K. Morokuma, D.K. Malick, A.D. Rabuck, K. Raghavachari, J.B. Foresman, J. Cioslowski, J.V. Ortiz, B.B. Stefanov, G. Liu, A. Liashenko, P. Piskorz, I. Komaromi, R. Gomperts, R.L. Martin, D.J. Fox, T. Keith, M.A. Al–Laham, C.Y. Peng, A. Nanayakkara, C. Gonzalez, M. Challacombe, P.M.W. Gill, B. Johnson, W. Chen, M.W. Wong, J.L. Andres, C. Gonzalez, M. Head–Gordon, E.S. Replogle, J.A. Pople, Gaussian, Inc., Pittsburgh PA, **1998**.
[26] A .D. Becke, A new Mixing of Hartree–Fock and Local Density–Functional Theories, *J. Chem. Phys.* **1993**, *98*, 1372–1377.
[27] C. Lee, W. Yang and R. G. Parr, Development of the Colle–Salvetti Correlation–Energy Formula Into a Functional of the Electron Density, *Phys. Rev. B* **1988**, *37*, 785–789.
[28] T. Müller and Y. Apeloig, Possible Strategies Toward the Elusive Tetraaminodisilene, *J. Am. Chem. Soc*. **2002**, *124*, 3457–3460.
[29] J. E. Carpenter and F. Weinhold, Analysis of the Geometry of the Hydroxymethyl Radical by the "Different Hybrids for Different Spins" Natural Bond Orbital Procedure, *J. Mol. Struct. (Theochem)* **1988**, *169*, 41–62; A.E. Reed, R.B. Weinstock and F. Weinhold, Natural Population Analysis, *J. Chem. Phys.* **1985**, *83*, 735–746.
[30] Structure of the digermene counterpart of compound **2** has similar geometrical features as **2** – butterfly bending of 48.4^{o} and 56.1^{o}. Detailed study and comparison with disilene molecules **1** and **2** with corresponding digermene molecules was not possible. All our attempts to locate ground state structure of *syn*– digermene conterpart of compound **1** failed, only structures having one imaginary frequency of vibration were found.
[31] A. G. Griesbeck, T. Deufel, G. Hohlneicher, R. Rebentisch and J. Steinwascher, Synthesis, Structure, and Properties of Twofold bridged Sesquinorbornenes, *Eur. J. Org. Chem.* **1998**, 1759–1762.
[32] T. A. Schmedake, M. Haaf, Y. Apeloig, T. Müller, S. Bukalov and R. West, Reversible Transformation between a Diaminodisylene and a Novel Disilene, *J. Am. Chem. Soc.* **1999**, *121*, 9479–9480.
[33] We again report all pyramidalization results in terms of the butterfly bending angle (ψ) which is defined in our earlier paper: D. Margetić, R.V. Williams and R.N. Warrener, Pyramidalized Olefins: A DFT Study of the Homosesquinorbornene and Sesquibicyclo[2.2.2]octene Nuclei, *J. Org. Chem.* **2003**, *68,* 9816–9190.
[34] B. Yates**,** Olefin Strain Energies and Platinum Complexes of Highly Pyramidalised Alkenes, *J. Organomet. Chem.* **2001**, *635*, 142–152.
[35] D. A. Hrovat and W. T. Borden, Ab Initio Calculations of the Olefin Strain Energies of Some Pyramidalized Alkenes, *J. Am. Chem. Soc.* **1988**, 4710–4718.
[36] K. Komatsu, Cyclic p–Conjugated Systems Annelated with Bicyclo[2.2.2]octene: Synthesis, Structures, and Properties, *Bull. Chem. Soc. Jpn.* **2001**, *74*, 407–409. Studies of properties of the cyclic π–conjugated systems annelated with bicyclo[2.2.2]octene showed that the π systems carrying a positive charge are remarkably stabilized due to the effective σ–π conjugation.
[37] T. Tsumuraya, S. A. Batcheller and S. Masamune, Strained–Ring and Double–Bond Systems Consisting of the Group 14 Elements Si, Ge, and Sn, *Angew. Chem. Int. Ed. Engl.* **1991**, *30*, 902–930.
[38] For comparison, experimental values for vertical ionization energies ($I_{v,j}$) of *syn*– and *anti*– sesquinorbornenes are 8.12 and 7.90 eV, respectively.
[39] M. E. Casida, C. Jamorski, K.C. Casida and K.D.R. Salahub, *J. Chem. Phys.* **1998**, *108*, 4439.
[40] K. Fukui, Theory of Orientation and Stereoselection, Springer, **1970**.
[41] D. Margetić, I. Antol and M. Eckert–Maksić, *J. Organomet. Chem.,* submitted
[42] B. Wrackemeyer, W. Milius, M. H. Bhatti and S. Ali, [4+2]Cycloadditions of Organometallic–substituted Siloles with Dimethyl Acetylenedicarboxylate and Tetracyanoethylene, *J. Organomet. Chem.* **2003**, *665*, 196–204.
[43] R. West, Chemistry of the Silicon–Silicon Double Bond, *Angew. Chem. Int. Ed. Engl.* **1987**, *99*, 1201–1211.

Biographies

Davor Margetić is research scientist working in Laboratory for Physical Organic Chemistry, Division of Organic Chemistry and Biochemistry, Ruđer Bošković Institute in Zagreb, Croatia.

Mario Vazdar is computational chemist working on his Ph.D. thesis under the supervision of Dr. Mirjana Eckert–Maksić.

Mirjana Eckert–Maksić is senior research scientist and head of Laboratory for Physical Organic Chemistry.